

## **PLGA-nano-encapsulated Disulfiram inhibits hypoxia-induced NFκB, cancer stem cells and targets glioblastoma *in vitro* and *in vivo***

Vinodh Kannappan<sup>ad†</sup>, Ying Liu<sup>b†\*\*</sup>, Zhipeng Wang<sup>a†</sup>, Karim Azar<sup>a†</sup>, Sathishkumar Kurusamy<sup>a\*\*</sup>, Rajagopal S Kilari<sup>a</sup>, Angel L Armesilla<sup>a</sup>, Mark R Morris<sup>a</sup>, Mohammad Najlah<sup>c</sup>, Peng Liu<sup>a\*\*</sup>, Xiu-wu Bian<sup>b\*</sup>, Weiguang Wang<sup>ad\*</sup>

<sup>a</sup>Faculty of Science & Engineering, University of Wolverhampton, Wolverhampton WV1 1LY, UK; <sup>b</sup>Institute of Pathology and Southwest Cancer Center, Third Military Medical University, China; <sup>c</sup>Faculty of Health, Education, Medicine and Social Care, Anglia Ruskin University, UK; <sup>d</sup>Disulfican Ltd, UK.

\*Corresponding authors, W Wang, Phone: +44-1902-322756; Email, [w.wang2@wlv.ac.uk](mailto:w.wang2@wlv.ac.uk); X-W Bian, Email: [bianxiuwu@263.net](mailto:bianxiuwu@263.net)

\*\*YL and PL's current affiliation: Barts Cancer Institute/Queen Mary University of London, UK; SK's current affiliation: University of Kent

<sup>†</sup>These authors contributed equally to this article.

**Running title:** PLGA-Disulfiram targets GBM *in vitro* and *in vivo*

**Key words:** Glioblastoma multiforme; NFκB; Disulfiram; PLGA; Cancer stem cells

**Abbreviations:** GSC: glioblastoma stem cell; DS: Disulfiram; DS-PLGA: poly lactic-co-glycolic acid nanoparticle-encapsulated DS; GBM: glioblastoma multiforme; CSC: cancer stem cell; ALDH: aldehyde dehydrogenase; EMT: epithelial-to-mesenchymal transition; HIF: hypoxia inducible factor; NFκB: nuclear factor kappa B; ROS: reactive oxygen species; Cu: copper(II); MTT: 3-(4,5-cimethylthiazol-2-yl)-2,5-diphenyl tetrazolium bromide; DDC: diethyldithiocarbamate; NS: neurosphere; SUS: suspension culture; TUNEL: terminal deoxyribonucleotidyl transferase-mediated dUTP nick end labeling assay; TMZ: temozolomide.

**Authors' Disclosures:** VK is employed by Disulfican Ltd and a visiting scientist in UoW; WW is Director of Disulfican Ltd and Professor in UoW. No disclosures from the other authors.

**Financial Support:** This study was supported by Research Institute in Healthcare Science/University of Wolverhampton PhD studentship; Innovate UK Jiangsu-UK

Industrial Challenge Programme (104022); Some key equipment was jointly funded by European Regional Developmental Fund, Smart Concept Fund, University of Wolverhampton and Disulfican Ltd.

**Authors' Contributions:**

**V Kannappan:** Performing all key experiments, formal analysis, writing original draft and editing; **Y Liu:** Performing key animal experiments and analysis; **Z Wang:** Compound formulation, PK experiments and analysis; **K Azar:** Performing some key in vitro experiments and analysis; **S Kurusamy:** Performing real-time RT-PCR experiments and analysis; **RS Kilari:** Performing some western blot experiments and analysis; **AL Armesilla:** Supervision; **MR Morris:** Supervision, data analysis and reviewing manuscript. **M Najlah:** Data analysis; **P Liu:** Performing some key experiments and analysis; **X Bian:** Conceptualization and supervision; **W Wang:** Conceptualization, supervision, writing, reviewing and editing manuscript.

## Abstract

Glioblastoma stem cell (GSC) is the major cause of glioblastoma multiforme (GBM) chemotherapy failure. Hypoxia is one of the determinants of GSC. NF $\kappa$ B plays a pivotal link between hypoxia and cancer stem cells (CSCs). Disulfiram (DS), an antialcoholism drug, has very strong NF $\kappa$ B-inhibiting and anti-CSC activity. In this study, the *in vitro* anti-GSC activity of DS and *in vivo* anti-GBM efficacy of poly lactic-co-glycolic acid nanoparticle-encapsulated DS (DS-PLGA) were examined. We attempt to elucidate the molecular network between hypoxia and GSCs, and also examined the anti-GSC activity of DS *in vitro* and *in vivo*. The influence of GSCs and hypoxia on GBM chemoresistance and invasiveness was studied in hypoxic and spheroid cultures. The molecular regulatory roles of NF $\kappa$ B, HIF1 $\alpha$  and HIF2 $\alpha$  were investigated using stably transfected U373MG cell lines. The hypoxia in neurospheres determines the cancer stem cell characteristics of the sphere-cultured GBM cell lines (U87MG, U251MG, U373MG). NF $\kappa$ B is located at a higher hierarchical position than HIF1 $\alpha$ /HIF2 $\alpha$  in hypoxic regulatory network and plays a key role in hypoxia-induced GSC characters. DS inhibits NF $\kappa$ B activity and targets hypoxia-induced GSCs. It showed selective toxicity to GBM cells, eradicates GSC and blocks migration and invasion at very low concentrations. DS-PLGA efficaciously inhibits orthotopic and subcutaneous U87MG xenograft in mouse models with no toxicity to vital organs.

## INTRODUCTION

Glioblastoma multiforme (GBM) is one of the most lethal and aggressive forms of the malignant adult brain tumor. Despite multimodal treatment including surgical resection with concurrent and adjuvant radiotherapy and chemotherapy, the prognosis of GBM is poor with the median survival time of only 14.6 months and less than 5% of GBM patients surviving for more than 2 years (1).

GBM manifests high intratumoural heterogeneity with a very small population of cells expressing cancer stem cell (CSC) markers, e.g. aldehyde dehydrogenase (ALDH), CD44, CD133, Sox2, Oct4 and Nanog, with epithelial-to-mesenchymal transition (EMT) trend (2,3). This population of cells has been clarified as glioblastoma stem cells (GSCs) which are quiescent, chemoresistant and metastatic (4,5). Studies indicate that GSCs, lodged in hypoxic niches, is a microenvironment inducible transient and reversible state rather than a permanent entity (6). As a heterogeneous tumor with an extensively hypoxic environment, GBM provides hypoxic niches for fostering and maintaining GSCs. Hypoxia inducible factors (HIFs) are the master transcriptional regulators induced by hypoxia (7). Nuclear factor-kappa B (NFκB) is a bridge linking inflammation, hypoxia and cancer (8,9). NFκB is an important chemoresistance-related transcription factor upregulating multiple genes related to inflammation, hypoxic response, EMT and anti-apoptotic signaling (10). Many human cancer cells and drug-resistant cancer cell lines possess high constitutive NFκB activity, which can be further induced by hypoxia (9). Ectopic overexpression of NFκB has been shown to result in inducing genes related to cancer cell stemness, EMT and anti-apoptosis (11-14). The relationship between HIFs and NFκB in coordinating the hypoxia induced GSC characters remains obscure. Understanding the molecular mechanisms behind hypoxia induced EMT and GSCs may facilitate development of new drugs for GBM therapeutics.

The demand of new drugs for GBM treatment is of clinical urgency but new drug development is a highly time and cash consuming procedure. There is a global trend

towards the repositioning of known drugs for new indications (15). Disulfiram (DS), a long-established alcohol-reversal drug, possesses excellent anticancer activity against a wide range of cancers including GBM with low toxicity to normal cells (13,16-19). DS also presents a synergistic activity and potentiates the cytotoxicity of conventional chemotherapy drugs and protects normal cells in kidney, gut and bone marrow *in vivo* whilst increasing the therapeutic index (13,19,20).

DS specifically inhibits the activity of ALDH, a functional marker of CSCs with reactive oxygen species (ROS) scavenging activity (21). It effectively eliminates CSCs and reverses chemoresistance (20-22). The cytotoxicity of DS is dependent on copper(II) (Cu) and other divalent transition metal elements (23,24). DS-metal complexes block the nuclear translocation of NF $\kappa$ B by inhibiting proteasome activation and I $\kappa$ B $\alpha$  degradation (17). The functional component of DS is diethyldithiocarbamate (DDC), which strongly chelates Cu to generate ROS and form the end product DDC-Cu. Both ROS and DDC-Cu induce cancer cell apoptosis (23,24). Therefore, the intact sulfhydryl group is essential for the reaction between DS and Cu. Only oral DS is currently available in clinic. Oral DS is quickly reduced to DDC in the gastrointestinal system. The sulfhydryl groups in DDC are instantly methylated and glucuronidated when DS is enriched in the liver. The methylated and glucuronidated DDC loses its Cu chelating function and cytotoxicity (24,25). The half-life of DS is less than 1 min in serum (16). This explains why anticancer activity of DS has been known for more than 30 years without successful and reproducible cancer therapeutic outcomes. We have demonstrated that using a nano-delivery system to protect the sulfhydryl group in DS can improve the anticancer efficacy of DS in breast, liver and lung cancer models (16,26).

Here, we demonstrate that NF $\kappa$ B plays pivotal roles in hypoxia-induced GSC traits. DS inhibits the NF $\kappa$ B pathway, targets GSCs and reverses chemoresistance *in vitro*. A strong *in vivo* anti-GBM efficacy was achieved by intravenous administration of a long-half-life circulating poly lactic-co-glycolic acid (PLGA) encapsulated DS (DS-PLGA) in both intracranial and subcutaneous mouse GBM models. Further study may translate DS-PLGA

into GBM treatment.

## Materials and Methods

### Cell lines and Reagents

The following human GBM cell lines U87MG ATCC (RRID:CVCL\_0022), U251MG (RRID:CVCL\_0021), and U373MG ATCC (RRID:CVCL\_2219) were purchased from ECACC (Porton Down, UK). The U373MG ATCC cell line is a derivative of the U251MG cell line. All human cell lines have been authenticated using STR profiling within the last three years and all experiments were performed with mycoplasma-free cells. DS, temozolomide (TMZ), copper chloride (CuCl<sub>2</sub>), copper gluconate (CuGlu), crystal violet, dichloromethane, poly-2-hydroxyethyl methacrylate (poly-HEMA) and bovine serum albumin (BSA) were from Sigma (Dorset, UK). DMEM medium and fetal calf serum (FCS) were supplied by Lonza (Wokingham, UK). Antibodies were purchased from Cell Signaling (Danvers, MA, USA: Ki67 and BAX), Abcam (Cambridge, UK: NFκBp65, IκBa, Bax, Bcl2, MMP-2, BMP4, BMP9, Sox2, Oct4, Nanog, E-Cadherin, N-Cadherin, Vimentin and ALDH1), BD Biosciences (Wokingham, UK) or Miltenyi Biotec (Bisley, UK) (CD44-FITC and CD133-FITC). Hypoxyprobe™-1 Plus kit was from Hypoxyprobe (Burlington, MA, USA). ALDEFLUOR was from Stemcell technologies (Cambridge, UK). Matrigel and cell culture inserts were purchased from Fisher (Loughborough, UK). The DS-PLGA was developed in our laboratory (16).

### Normoxic and Hypoxic Cell culture

The GBM cell lines were cultured under normoxia (20% oxygen) or hypoxia (1% oxygen) and maintained in DMEM supplemented with 10% FCS, 2mM L-Glutamine, 50 units/ml penicillin, and 50 µg/ml streptomycin. Cells were cultured under normoxia or hypoxia in parallel for 5 days before further experiments. The hypoxic culture was performed in a Panasonic Hypoxia Incubator (Panasonic Biomedical, Loughborough, UK).

### *In vitro* spheroid culture

Cells were cultured in ultra-low adherence poly-HEMA coated T25 flasks at a cell density of 20,000 cells/mL. Neurosphere (NS) was grown in neural stem cell medium [serum-free DMEM-F12 supplemented with B27 and N2 serum replacement (Invitrogen), 0.3% glucose (Sigma), 10 ng/ml epidermal growth factor (Sigma), 10 ng/ml basic fibroblasts growth factor (R&D System, Abingdon, UK), 20 mg/ml insulin (Sigma), 2 mg/ml heparin (Sigma)]. The group of suspension culture (SUS) was performed in normal DMEM

supplemented with 10% serum. The cells were incubated at 37°C for 7 days, before further analysis, with necessary media replenishment every 3 days.

### **Detection of hypoxia in cell culture**

The Hypoxyprobe Kit was used following the manufacturer's protocol. For immunocytochemistry assay, the attached cells (ATT) were cultured at normoxic or hypoxic condition for 72 hours and co-cultured with Hypoxyprobe reagent overnight. The NS and SUS cells were co-cultured with Hypoxyprobe overnight and cytopspined at 800 rpm for 3 min to spread the spheres onto Polylysine-coated slides (VWR, Lutterworth, UK). The cells were fixed and stained with FITC-conjugated anti-hypoxyprobe MAb and imaged using a confocal microscope. For quantification of hypoxic cells, the cells were stained with Hypoxyprobe and subjected to flow cytometric analysis. The hypoxic population was detected using a FACS Calibur flow cytometer with 488-nm blue laser and standard FITC 530/30 nm bandpass filter.

### **Flow cytometric analysis of CSC markers**

The trypsinised cells ( $2.5 \times 10^5$ ) were analysed with corresponding CSC markers. ALDH activity was measured by staining with ALDH substrate. The CD133 and CD44 cell surface marker were detected by FITC-conjugated anti-CD133 and anti-CD44 antibodies. The cells were examined using BD FACS Calibur and Cell Quest Pro software.

### ***In vitro* cytotoxicity assay**

The methodology of MTT assay for the normoxia cultured cells has been described previously (22). To determine the effect of hypoxia on drug sensitivity, the cells were cultured in 1% oxygen at a cell density of  $5 \times 10^3$  cells/well in 96-well plate for 4 days and exposed to anticancer drugs for another 72 h before 3-(4,5-dimethylthiazol-2-yl)-2,5-diphenyl tetrazolium bromide (MTT) assay with a parallel MTT assay in normoxia. The NS and SUS spheres were trypsinised and re-cultured in poly HEMA-coated 96-well flat bottom plates in their corresponding culture medium at a cell density of  $5 \times 10^3$  cells/well overnight. After exposure to drugs for 72 hours, the cells were subjected to a

standard MTT assay. The NS and SUS cells were centrifuged at 800 rpm for 5 mins before MTT assay.

### **Western blot analysis of proteins**

The whole and nuclear protein was extracted from normoxia, hypoxia, NS and SUS cultured GBM cells with RIPA buffer, quantified and separated by SDS PAGE. The proteins were blotted onto PVDF membrane (Fisher Sci, Loughborough, UK), blocked with 5% non-fat milk and incubated with appropriate primary and secondary antibodies of target proteins.

### **Stable transfection of U373MG cell line with NFκBp65, HIF1α and HIF2α**

U373MG cells ( $2.5 \times 10^5$ /well) were cultured in 35-mm dishes until 70% confluent, and Lipofectamine 2000 Superfect (Qiagen, West Sussex, United Kingdom) was used to transfect pcDNA3.1(+) (Invitrogen, Paisley, UK), pcDNA3.1/Hygro/NFκBp65, pCMV6-Neo/HIF1α, pCMV6-Neo/HIF2α (Origene, Rockville, MD, USA). The successfully transfected clones were selected in relevant antibiotics.

### ***In vitro* migration and invasion assay**

The migration and invasion assays were performed using cell culture inserts (Fisher Sci) coated with or without Matrigel (BD Bioscience). Cells ( $5 \times 10^4$ ) were resuspended in 200 μl of serum-free DMEM and placed in the upper chamber of the insert. The lower chamber was filled with medium containing 10% FCS. After 16 hours incubation at 37°C, migrated cells were fixed by methanol and stained in 0.5% crystal violet. Cells were imaged and counted under a microscope.

### **Quantitative real time RT-PCR (qRT-PCR)**

qRT-PCR was performed using Taqman™ assays. RNA was extracted using an RNA purification kit (Norgen, Canada) following the manufacturer's instructions and reverse transcribed into cDNA (Multiscribe Reverse Transcriptase, Applied Biosystems). A QuantStudio 6 Flex Real-Time PCR system (Applied Biosystems) was used for qPCR experiments. Gene expression levels were normalised to control genes (GAPDH and

HPRT1) and calculated according to the  $\Delta\Delta\text{CT}$  method.

### **Luciferase reporter gene assay**

The cells ( $1 \times 10^4$ /well) were cultured in 96-well plates overnight. The NF $\kappa$ B (pNF $\kappa$ B $\alpha$ -Luc, BD Biosciences) and HRE (Promega, Southampton, UK) luciferase reporter vectors and pGL3-Basic (Promega) were co-transfected with pSV40-Renilla (Promega) DNA. Forty-eight hours after transfection, the luciferase activity was determined using Dual Luciferase Assay reagents (Promega) according to the manufacturer's instructions. The relative luciferase activity was calculated (26).

### **Immunohistochemistry and H&E staining**

The sections from paraffin embedded tumor and normal tissues were stained with primary antibodies [Ki67, Bax, NF $\kappa$ Bp65 and ALDH1 (1:200)] then biotinylated secondary antibody and followed by incubation in ABC reagent (DAKO Labs, Cambridgeshire, UK). For H&E staining, the paraffin-embedded sample slides were stained with hematoxylin and eosin and the slides were mounted with coverslips using Permount (Fisher Sci, Loughborough, UK).

### **Terminal deoxyribonucleotidyl transferase-mediated dUTP nick end labeling (TUNEL) assay**

Tumor tissues were paraffin embedded and stained according to the instruction of the manufacturer (Roche, West Sussex, UK). Briefly, the slides were incubated with TdT Enzyme, Stop/Wash Buffer, antidigoxigenin, and then stained with peroxidase substrate and incubated in ABC reagent. Finally, the slide was mounted with 3,3'-diaminobenzidine and visualized under a light microscope.

### **Pharmacokinetic study and *in vivo* anti-GBM xenograft experiments**

The animal experiments were reviewed and approved by the Ethical Committee of Third Military Medical University, China and University of Wolverhampton, UK. Rats (5/group) were injected with DS or DS-PLGA (250mg/kg) through a tail vein. Blood samples were collected at 0.25, 0.5, 1, 2, 4, 8 min for the DS group and at 5, 10, 20, 40, 60, 120, 180

min for the DS-PLGA group. The plasma (500  $\mu$ l) was separated and mixed with methanol (250  $\mu$ l). After vigorously shaking and centrifuging (10,000 rpm, 15 min), the DS concentration in the supernatant was determined by HPLC as described elsewhere (16). The intracranial GBM model was developed as previously described (27). Briefly, the five-week-old female BALB/c Nu/Nu mice were anesthetized. The U87MG-Luciferase-GFP cells ( $2 \times 10^5/5 \mu$ l PBS) were injected into the brain using a 25 $\mu$ l micro-syringe. After 10 days, the animals were treated with empty PLGA or DS-PLGA (10mg/kg iv) plus CuGlu (6mg/kg po) 3/week for 4 weeks. For the subcutaneous GBM model, U87MG cells ( $5 \times 10^6$ ) were injected into the front flank of BALB/c Nu/Nu mice. When the tumor volume (V) reached  $\sim 200 \text{mm}^3$ , the tumor bearing mice were subjected to the above treatment. The xenograft size was recorded twice per week. The tumor volume was calculated by the following formula:  $V = (L \times W^2) \times 0.5$ , where L is the length and W is the width of the tumor. After 4 weeks, the animals were sacrificed. The tumors were removed, photographed and subjected to further analysis.

### **Statistical analysis**

Student's t-test and one-way ANOVA were used in this study.  $p < 0.05$  and  $< 0.01$  were considered statistically significant and highly significant respectively.

### **Data availability statement**

The data generated in this study are available within the article and its supplementary data files.

## Results

### **Hypoxia, stemness, NFkB activation and TMZ resistance were detected in both neurosphere and suspension cultured GBM cells.**

Characteristic spheres were formed in both serum-free neurosphere (NS) and serum-rich suspension (SUS) culturing conditions (Fig. 1A). All the sphere cells express high stem cell (Fig. 1B) and embryonic stem cell markers (Fig. 1C). Overexpression of N-cadherin, vimentin and downregulation of E-cadherin were detected in NS and SUS cells indicating the presence of EMT in the sphere cells (Fig. 1D). Significant TMZ resistance was detected when the sphere cells were exposed to TMZ for 72 hours and subjected to sphere reformation and MTT cytotoxicity assay (Fig. 1A, Table S1 and S2).

Hypoxyprobe staining showed hypoxic population in the core region of both NS and SUS (Fig. 1E). A high proportion of hypoxic cells were detected in NS and SUS cells using flow cytometry (Fig. 1F). Further evidence of the hypoxic condition in NS and SUS cells was shown by the overexpression of HIF1 $\alpha$  and HIF2 $\alpha$  proteins (Fig. 1G). Overexpression of NFkBp65 was detected in the sphere cells (Fig. 1H).

### **Hypoxia induces stemness, NFkB activation, EMT and TMZ resistance in GBM cells.**

To confirm the link between hypoxia and GSC phenotypes, we cultured monolayer GBM cells under hypoxia. The cellular hypoxia was confirmed by Hypoxyprobe staining (Fig. 2A, B) and overexpression of HIF1 $\alpha$  and HIF2 $\alpha$  proteins (Fig. 2C). The hypoxia culture induces high levels of GSC and embryonic stem cell markers (Fig. 2D, E). The hypoxic GBM cells are significantly resistant to TMZ (Fig. 2F). The overexpression of Bcl2 and downregulation of Bax indicate that hypoxia activates anti-apoptotic pathways (Fig. 2G). Hypoxia-induced EMT was confirmed by the overexpression of CD44, vimentin, N-cadherin, downregulation of E-cadherin (Fig. 2D, H) and overexpression of mRNA from EMT and metastasis related genes (Fig. S1). Increased migration and invasion abilities

were manifested in the hypoxia cultured GBM cells (Fig. 2I, J; Table S3). Together, the above findings indicate that hypoxia induces stemness, EMT and chemoresistance in GBM cells. Similar to spheroid cultures, the high expression of NFκBp65 protein and its nuclear translocation were also detected in the hypoxia cultured cells (Fig. 2K).

### **The regulatory relationship of NFκB, HIF1α and HIF2α in GBM cells.**

HIFs and NFκB are hypoxia-induced genes responsible for EMT and CSC traits(14,28). The regulatory relationship between HIFs and NFκB is still not clear. To establish which one of these three factors is on the central regulatory position in hypoxia response, we stably transfected U373MG cells with NFκBp65, HIF1α and HIF2α. The successful transfected clones were confirmed by Western blot and luciferase reporter gene assay (Fig. 3A – F). The NFκBp65 transfected clones express high levels of HIF1α and HIF2α proteins (Fig. 3G) and mRNAs (Fig. S2) and possess high HRE transcriptional activity (Fig. 3H). In contrast, HIF1α and HIF2α transfected clones did not show significant NFκB up-regulation at mRNA (Fig. S2), protein (Fig. 3I, K) and transcription (Fig. 3J, L) levels. The expression of HIF2α mRNA was upregulated by HIF1α transfection but not vice versa (Fig. S2). Therefore, NFκB may be located at a higher hierarchical position than HIF1α and HIF2α in hypoxia response gene network.

### **The effect of NFκB and HIFs on stemness, EMT, TMZ resistance and invasiveness in GBM cells.**

Next, we examined the effect of NFκB and HIFs on EMT and stemness in GBM cells. The NFκBp65, HIF1α and HIF2α transfected clones express higher levels of GSC (Fig. 4A) and embryonic stem cell (Fig 4B) markers. The mRNA and protein of EMT related genes were detected in the transfected clones (Fig. 4C, D). The NFκBp65 and HIF2α but not HIF1α transfected clones are significantly resistant to TMZ (Fig. 4E). We also examined the migration and invasion abilities, one of the most common features of EMT (29), in the transfected cell lines. All of the NFκBp65, HIF1α and HIF2α transfected cell lines possess significantly higher migration and invasion activity (Fig. 4F-H; Table S4). Some

metastasis related genes are overexpressed in these cell lines (Fig. 4D). These data indicate that all of these three genes promote the invasiveness of GBM but only NF $\kappa$ B and HIF2 $\alpha$  are responsible for TMZ resistance.

### **Disulfiram inhibits hypoxia-induced GSC and EMT phenotypes *in vitro***

Hypoxic cells remain sensitive to DS (Fig. 5A) although they are significantly resistant to TMZ. DS and Cu block the sphere reformation in NS and SUS cultures. The DS or Cu alone had no effect on sphere reformation indicating the essential requirement of Cu in the function of DS against GSCs (Fig. 5B, C; Table S2). The GSC markers induced by spheroid and hypoxia culture were blocked by DS/Cu (Fig. 5D, E, S3, S4). DS/Cu inhibited the migration and invasion of GBM cell lines at an extremely low concentration (25nM) (Fig. 5F, G; Table S3). NF $\kappa$ B is a key player in GSC and EMT. The expression of NF $\kappa$ Bp65 protein in hypoxia and sphere cultured GBM cells was inhibited by DS/Cu (Fig. 5H). DS/Cu treatment enhanced and inhibited the expression of Bax and Bcl2 respectively (Fig. 5H).

### **DS-PLGA extends the half-life of DS *in vivo* and suppresses GBM in orthotopic and subcutaneous GBM mouse models**

To overcome the very short half-life of DS in the bloodstream (16,30), we used a DS-PLGA formulation (16) to deliver DS intravenously in a mouse model. The half-life of DS-PLGA in rat was 13.4 minutes (Table S5) whilst the free DS was immediately undetectable after injection.

The *in vivo* efficacy of DS-PLGA was assessed in both intracranial and sub-cutaneous models. After 4 weeks treatment, DS-PLGA/Cu significantly reduced the sizes of the intracranial and subcutaneous tumors and the tumor weight in subcutaneous injected mice (Fig. 6A - C). These results indicate that the PLGA encapsulation delivers the intact DS to GBM tissues. The TUNEL staining indicated apoptosis induced by DS-PLGA/Cu *in vivo* (Fig. 6D). DS-PLGA/Cu treatment inhibited the expression of NF $\kappa$ Bp65, ALDH and Ki67 expression in the GBM xenografts (Fig. 6E). No toxic effect on vital organs were

observed and mouse body weight was maintained (Fig. 6F, G).

## Discussion

Investigation and unveiling of molecular mechanisms of GSC induced chemoresistance and invasiveness (4,5) will likely facilitate the development of novel and efficacious therapies for GBM patients. Since Reynolds and Weiss successfully isolated normal neural stem cells using sphere-forming culture in growth factor-supplemented serum-free medium (31), this system has been widely adapted for *in vitro* culture of GSCs. It has been generally believed that serum-free and growth factors rich medium are essential for maintenance of anchorage-independent proliferation and stemness. Our study manifested that GBM cells form neurospheres in both serum-rich and serum-free media which express comparable levels of GSC markers (Fig. 1B, C) and are significantly resistant to TMZ (Fig. 1A and Table S1). Similar findings were reported previously (26,32,33). EMT and CSCs are inextricably linked microenvironment-determined transient epigenetic phenomena (34), which were detected in NS and SUS cells (Fig. 1B, D). Hypoxia is a central determinant of the stem cell niche (35), which is relevant to GBM as these tumors have significantly lower intratumoral oxygen concentration than normal brain tissues (36). In line with our previous findings in breast cancer (26), the core regions of neurospheres contain a high proportion of hypoxic cells (Fig. 1E, F) which express high levels of HIF1 $\alpha$ , HIF2 $\alpha$  and NF $\kappa$ Bp65 (Fig. 1G, H), the key factors induced by inflammation and hypoxia (7,8). The GBM cells cultured in hypoxia produce essential growth factors (EGF and bFGF) (37). Our results suggest that the GSC traits may be determined by the hypoxic microstructure of the spheroid culture rather than the medium and the selective medium may not be essential for the *in vitro* GSC culture. In contrast, the conventional serum-containing medium may better mimic the *in vivo* pathophysiological conditions and more suitable for *in vitro* GSC study.

The interconversion of CSCs and non-CSCs is a common phenomenon driven by environmental stimuli (2,3). As such, the GSC and non-GSC cells are mutable cellular traits determined by oxygen levels in the microenvironment (35). Hypoxia cultured cells

grown as a monolayer expressed high levels of GSC and embryonic stem cell markers and were markedly resistant to TMZ (Fig. 2D-F). A high proportion of both sphere- and hypoxia-cultured cells overexpressed CD44, N-cadherin, vimentin and some key EMT markers whereas, E-cadherin was downregulated (Fig. 1B, 1D, 2H; Fig. S1). These results indicate hypoxia induces EMT in these cells. EMT is responsible for cancer cell migration, invasion and metastasis (29). The hypoxia-cultured cells showed higher migration and invasion abilities (Fig. 2I, J; Table S3).

Overexpression of HIF1 $\alpha$ , HIF2 $\alpha$  and NF $\kappa$ Bp65 was detected in both sphere- and hypoxia-cultured GBM cells (Fig. 1G, 1H, 2C, 2K). These transcription factors are related to dedifferentiation and maintenance of GSCs (38). The stably transfected U373MG models were used to elucidate the hierarchical relationship among these three genes. NF $\kappa$ Bp65 transfection induced HIF1 $\alpha$  and HIF2 $\alpha$  protein, mRNA expression and HRE activity but not vice versa (Fig. 3G-M, S2). NF $\kappa$ B, HIF1 $\alpha$  and HIF2 $\alpha$  transfected cells express some key EMT transcription factors (Fig. 4C, D). NF $\kappa$ B may manipulate the hypoxia-induced activation of HIF1 $\alpha$  and HIF2 $\alpha$  via binding to the  $\kappa$ B-sites on their promoter regions (39). HIF1 $\alpha$  transfected clones overexpressed HIF2 $\alpha$  but not vice versa (Fig. S2). Although all of the HIF1 $\alpha$ , HIF2 $\alpha$  and NF $\kappa$ Bp65 transfected clones overexpress GSC and EMT markers, only NF $\kappa$ Bp65 and HIF2 $\alpha$  transfected cells are resistant to TMZ (Fig. 4E). This is consistent with previous reports that HIF1 $\alpha$  mainly regulates acute hypoxia induced cell responses. In contrast, HIF2 $\alpha$  is responsible for chronic hypoxia which induces GSC and EMT traits (40,41). HIF1 $\alpha$  may counterbalance the drug resistant effect of HIF2 $\alpha$  (42). All of these three genes induce the expression of key EMT and metastasis related genes and promote GBM cell migration and invasion (Fig. 4C, D, F-H; Table S4).

In line with our previous studies (16,22,24,26), DS targets NF $\kappa$ B and reverses hypoxia induced cancer metastasis/chemoresistance in a Cu-dependent manner (Fig. 5A-C, 5F, 5G). DS/Cu abolished GSC markers and completely blocked neurosphere reformation ability (Fig. 5B - E). Intracranial metastasis is the major cause of GBM recurrence

(43,44). DS blocked GBM cell migration and invasion at an extremely low concentration (25nM). In combination with radiotherapy, DS may effectively improve the current therapeutic outcomes of GBM.

The very short half-life of DS in the bloodstream is the key limit for its efficacy as cancer therapeutics. The DS-PLGA has a significantly longer half-life (Table S5 and(16)) and can successfully deliver intact DS to cancer tissues. The low molecular weight (296) and high lipophilicity facilitate DS to penetrate GBM tissues. The DS-PLGA/Cu showed very strong *in vivo* anti-GBM efficacy in both intracranial and subcutaneous mouse models. It inhibited NF $\kappa$ B and ALDH expression in GBM tissues. No systemic toxic effect of DS-PLGA/Cu on vital organs (kidney, liver, lung, spleen and brain) and no mouse body weight loss was observed. The intracranial metastasis is the major cause of postoperative relapse of GBM, although local drug delivery using BCNU/wafer marginally improved the survival time, the vulnerability of brain tissue to BCNU hinders its success in GBM treatment (45). DS showed selective toxicity in cancer cells (26). The migration/invasion inhibiting concentration (25nM) is significantly lower than its toxic concentration. DS-PLGA may potentially be locally delivered using convection-enhanced delivery (46) or wafer formulation in GBM treatment. Nevertheless, our results suggest that repurposing DS through a novel type of delivery system that prolongs its plasma half-life offers new possible therapeutic options for the treatment of GBM.

### **Acknowledgements**

We would like to express our great thanks to Professor Andrew Pollard (Chairman/Director, Disulfican Ltd) for his significant contribution to Innovate UK-Jiangsu grant application and project management. We are also immensely grateful to Professor Patrick Ball and Dr Hana Morrissey for their carefully reading and very constructive comments on an earlier version of this manuscript.

## References

1. Darefsky AS, King JT, Jr., Dubrow R. Adult glioblastoma multiforme survival in the temozolomide era: a population-based analysis of Surveillance, Epidemiology, and End Results registries. *Cancer* **2012**;118(8):2163-72 doi 10.1002/cncr.26494.
2. Mani SA, Guo W, Liao MJ, Eaton EN, Ayyanan A, Zhou AY, *et al.* The epithelial-mesenchymal transition generates cells with properties of stem cells. *Cell* **2008**;133(4):704-15 doi 10.1016/j.cell.2008.03.027.
3. Batlle E, Clevers H. Cancer stem cells revisited. *Nat Med* **2017**;23(10):1124-34 doi 10.1038/nm.4409.
4. Singh SK, Hawkins C, Clarke ID, Squire JA, Bayani J, Hide T, *et al.* Identification of human brain tumour initiating cells. *Nature* **2004**;432(7015):396-401.
5. Cheray M, Begaud G, Deluche E, Nivet A, Battu S, Lalloue F, *et al.* Cancer Stem-Like Cells in Glioblastoma. In: De Vleeschouwer S, editor. *Glioblastoma*. Brisbane (AU)2017.
6. Zipori D. The nature of stem cells: state rather than entity. *Nat Rev Genet* **2004**;5(11):873-8 doi 10.1038/nrg1475.
7. Keith B, Johnson RS, Simon MC. HIF1alpha and HIF2alpha: sibling rivalry in hypoxic tumour growth and progression. *Nat Rev Cancer* **2011**;12(1):9-22 doi 10.1038/nrc3183.
8. Clevers H. At the crossroads of inflammation and cancer. *Cell* **2004**;118(6):671-4.
9. D'Ignazio L, Rocha S. Hypoxia Induced NF-kappaB. *Cells* **2016**;5(1) doi 10.3390/cells5010010.
10. Soubannier V, Stifani S. NF-kappaB Signalling in Glioblastoma. *Biomedicines* **2017**;5(2) doi 10.3390/biomedicines5020029.
11. Wang W, Cassidy J. Constitutive nuclear factor-kappa B mRNA, protein overexpression and enhanced DNA-binding activity in thymidylate synthase inhibitor-resistant tumour cells. *Br J Cancer* **2003**;88(4):624-9.
12. Wang W, Cassidy J, O'Brien V, Ryan KM, Collie-Duguid E. Mechanistic and predictive profiling of 5-Fluorouracil resistance in human cancer cells. *Cancer Res* **2004**;64(22):8167-76.
13. Guo X, Xu B, Pandey S, Goessl E, Brown J, Armesilla AL, *et al.* Disulfiram/copper complex inhibiting NFkappaB activity and potentiating cytotoxic effect of gemcitabine on colon and breast cancer cell lines. *Cancer Lett* **2010**;291(1):104-13.
14. Prasad S, Ravindran J, Aggarwal BB. NF-kappaB and cancer: how intimate is this relationship. *Mol Cell Biochem* **2010**;336(1-2):25-37 doi 10.1007/s11010-009-0267-2.
15. Pushpakom S, Iorio F, Eyers PA, Escott KJ, Hopper S, Wells A, *et al.* Drug repurposing: progress, challenges and recommendations. *Nat Rev Drug Discov* **2018** doi 10.1038/nrd.2018.168.
16. Wang Z, Tan J, McConville C, Kannappan V, Tawari PE, Brown J, *et al.* Poly lactic-co-glycolic acid controlled delivery of disulfiram to target liver cancer stem-like cells. *Nanomedicine* **2017**;13(2):641-57 doi 10.1016/j.nano.2016.08.001.
17. Chen D, Cui QC, Yang H, Dou QP. Disulfiram, a clinically used anti-alcoholism drug and copper-binding agent, induces apoptotic cell death in breast cancer cultures and xenografts via inhibition of the proteasome activity. *Cancer Res* **2006**;66(21):10425-33.
18. Brar SS, Grigg C, Wilson KS, Holder WD, Jr., Dreau D, Austin C, *et al.* Disulfiram inhibits

- activating transcription factor/cyclic AMP-responsive element binding protein and human melanoma growth in a metal-dependent manner in vitro, in mice and in a patient with metastatic disease. *Mol Cancer Ther* **2004**;3(9):1049-60.
19. Lun X, Wells JC, Grinshtein N, King JC, Hao X, Dang NH, *et al.* Disulfiram when Combined with Copper Enhances the Therapeutic Effects of Temozolomide for the Treatment of Glioblastoma. *Clin Cancer Res* **2016**;22(15):3860-75 doi 10.1158/1078-0432.CCR-15-1798.
  20. Liu P, Kumar IS, Brown S, Kannappan V, Tawari PE, Tang JZ, *et al.* Disulfiram targets cancer stem-like cells and reverses resistance and cross-resistance in acquired paclitaxel-resistant triple-negative breast cancer cells. *Br J Cancer* **2013**;109(7):1876 - 85.
  21. Triscott J, Pambid MR, Dunn SE. Bullseye: Targeting cancer stem cells to improve the treatment of gliomas by repurposing Disulfiram. *Stem Cells* **2015** doi 10.1002/stem.1956.
  22. Liu P, Brown S, Goktug T, Channathodiyil P, Kannappan V, Hugnot JP, *et al.* Cytotoxic effect of disulfiram/copper on human glioblastoma cell lines and ALDH-positive cancer-stem-like cells. *Br J Cancer* **2012**;107(9):1488-97.
  23. Tawari PE, Wang Z, Najlah M, Tsang CW, Kannappan V, Liu P, *et al.* The cytotoxic mechanisms of disulfiram and copper(ii) in cancer cells. *Toxicol Res (Camb)* **2015**;4(6):1439-42 doi 10.1039/c5tx00210a.
  24. Butcher K, Kannappan V, Kilari RS, Morris MR, McConville C, Armesilla AL, *et al.* Investigation of the key chemical structures involved in the anticancer activity of disulfiram in A549 non-small cell lung cancer cell line. *BMC Cancer* **2018**;18(1):753 doi 10.1186/s12885-018-4617-x.
  25. Tawari PEW, Z.; Najlah, M.; Tsang, C. W.; Kannappan, V.; Liu, P.; McConville, C.; He, B.; Armesilla, A. L.; Wang, W. The cytotoxic mechanisms of disulfiram and copper(II) in cancer cells. *Toxicology Research* **2015**;4:1439 - 42.
  26. Liu P, Wang Z, Brown S, Kannappan V, Tawari PE, Jiang J, *et al.* Liposome encapsulated Disulfiram inhibits NFκB pathway and targets breast cancer stem cells in vitro and in vivo. *Oncotarget* **2014**;5(17):7471 - 85.
  27. Ping YF, Yao XH, Chen JH, Liu H, Chen DL, Zhou XD, *et al.* The anti-cancer compound Nordy inhibits CXCR4-mediated production of IL-8 and VEGF by malignant human glioma cells. *J Neurooncol* **2007**;84(1):21-9 doi 10.1007/s11060-007-9349-8.
  28. Mannello F, Medda V, Tonti GA. Hypoxia and neural stem cells: from invertebrates to brain cancer stem cells. *Int J Dev Biol* **2011**;55(6):569-81 doi 10.1387/ijdb.103186fm.
  29. Chaffer CL, San Juan BP, Lim E, Weinberg RA. EMT, cell plasticity and metastasis. *Cancer Metastasis Rev* **2016**;35(4):645-54 doi 10.1007/s10555-016-9648-7.
  30. Johansson B. A review of the pharmacokinetics and pharmacodynamics of disulfiram and its metabolites. *Acta Psychiatr Scand Suppl* **1992**;369:15-26.
  31. Reynolds BA, Weiss S. Generation of neurons and astrocytes from isolated cells of the adult mammalian central nervous system. *Science* **1992**;255(5052):1707-10.
  32. Hong X, Chedid K, Kalkanis SN. Glioblastoma cell line-derived spheres in serum-containing medium versus serum-free medium: a comparison of cancer stem cell properties. *Int J Oncol* **2012**;41(5):1693-700 doi 10.3892/ijo.2012.1592.
  33. Min SO, Lee SW, Bak SY, Kim KS. Ideal sphere-forming culture conditions to maintain pluripotency in a hepatocellular carcinoma cell lines. *Cancer Cell Int* **2015**;15:95 doi 10.1186/s12935-015-0240-y.

34. Shibue T, Weinberg RA. EMT, CSCs, and drug resistance: the mechanistic link and clinical implications. *Nat Rev Clin Oncol* **2017**;14(10):611-29 doi 10.1038/nrclinonc.2017.44.
35. Colwell N, Larion M, Giles AJ, Seldomridge AN, Sizdahkhani S, Gilbert MR, *et al.* Hypoxia in the glioblastoma microenvironment: shaping the phenotype of cancer stem-like cells. *Neuro Oncol* **2017**;19(7):887-96 doi 10.1093/neuonc/now258.
36. Beppu T, Kamada K, Yoshida Y, Arai H, Ogasawara K, Ogawa A. Change of oxygen pressure in glioblastoma tissue under various conditions. *J Neurooncol* **2002**;58(1):47-52.
37. Li G, Chen Z, Hu YD, Wei H, Li D, Ji H, *et al.* Autocrine factors sustain glioblastoma stem cell self-renewal. *Oncol Rep* **2009**;21(2):419-24.
38. Schwitalla S, Fingerle AA, Cammareri P, Nebelsiek T, Goktuna SI, Ziegler PK, *et al.* Intestinal tumorigenesis initiated by dedifferentiation and acquisition of stem-cell-like properties. *Cell* **2013**;152(1-2):25-38 doi 10.1016/j.cell.2012.12.012.
39. Bhat KPL, Balasubramaniyan V, Vaillant B, Ezhilarasan R, Hummelink K, Hollingsworth F, *et al.* Mesenchymal differentiation mediated by NF-kappaB promotes radiation resistance in glioblastoma. *Cancer Cell* **2013**;24(3):331-46 doi 10.1016/j.ccr.2013.08.001.
40. Holmquist-Mengelbier L, Fredlund E, Lofstedt T, Noguera R, Navarro S, Nilsson H, *et al.* Recruitment of HIF-1alpha and HIF-2alpha to common target genes is differentially regulated in neuroblastoma: HIF-2alpha promotes an aggressive phenotype. *Cancer Cell* **2006**;10(5):413-23 doi 10.1016/j.ccr.2006.08.026.
41. Bar EE. Glioblastoma, cancer stem cells and hypoxia. *Brain Pathol* **2011**;21(2):119-29 doi 10.1111/j.1750-3639.2010.00460.x.
42. Bordji K, Grandval A, Cuhna-Alves L, Lechapt-Zalcman E, Bernaudin M. Hypoxia-inducible factor-2alpha (HIF-2alpha), but not HIF-1alpha, is essential for hypoxic induction of class III beta-tubulin expression in human glioblastoma cells. *FEBS J* **2014**;281(23):5220-36 doi 10.1111/febs.13062.
43. Ostrom QT, Bauchet L, Davis FG, Deltour I, Fisher JL, Langer CE, *et al.* The epidemiology of glioma in adults: a "state of the science" review. *Neuro Oncol* **2014**;16(7):896-913 doi 10.1093/neuonc/nou087.
44. Lim M, Xia Y, Bettgowda C, Weller M. Current state of immunotherapy for glioblastoma. *Nat Rev Clin Oncol* **2018**;15(7):422-42 doi 10.1038/s41571-018-0003-5.
45. Bregy A, Shah AH, Diaz MV, Pierce HE, Ames PL, Diaz D, *et al.* The role of Gliadel wafers in the treatment of high-grade gliomas. *Expert Rev Anticancer Ther* **2013**;13(12):1453-61 doi 10.1586/14737140.2013.840090.
46. Kunwar S, Chang S, Westphal M, Vogelbaum M, Sampson J, Barnett G, *et al.* Phase III randomized trial of CED of IL13-PE38QQR vs Gliadel wafers for recurrent glioblastoma. *Neuro Oncol* **2010**;12(8):871-81 doi 10.1093/neuonc/nop054.

## Figure Legends

**Fig. 1** Hypoxia, EMT/stemness, TMZ resistance and overexpression of NF $\kappa$ Bp65 were detected in spheroid cells. A. Morphology of TMZ treated attach (ATT), neurosphere (NS) and suspension-cultured (SUS) GBM cells. B. Flow cytometric analysis of the expression of CD133, CD44 and ALDH activity (mean  $\pm$  SD; n=3). C and D. WB analysis of embryonic stem and EMT-related proteins. E. Hypoxic cells were detected by Hypoxyprobe and FITC-conjugated anti-Hypoxyprobe MAb staining (green, cytoplasm). The nuclei were counterstained by PI (red). F. Flow cytometric analysis of Hypoxyprobe-stained cells (mean  $\pm$  SD; n=3). G and H. WB of HIF1 $\alpha$  and HIF2 $\alpha$  (G, nuclear protein) and NF $\kappa$ Bp65 (H) protein expression.  $\beta$ -Actin and Nucleolin were used as house-keeping control. \*\*p<0.01.

**Fig. 2** EMT/stemness, TMZ resistance, invasiveness and NF $\kappa$ B status detected in hypoxia-cultured GBM cells. A. Images of Hypoxyprobe-stained cells. Hypoxic cells were detected by Hypoxyprobe and FITC-conjugated anti-Hypoxyprobe MAb staining (green, cytoplasm). The nuclei were counterstained by PI (red). B. Flow cytometric analysis of Hypoxyprobe-stained cells (mean  $\pm$  SD; n=3). C. WB of HIF1 $\alpha$  and HIF2 $\alpha$  (nuclear protein). D. Flow cytometric analysis of CD133, CD44 and ALDH status in normoxia- and hypoxia-cultured cells (mean  $\pm$  SD; n=3). E. WB of embryonic proteins in normoxia- and hypoxia-cultured cells. F. IC<sub>50</sub> of TMZ in normoxia- and hypoxia-cultured cells (mean  $\pm$  SD; n=3). G. WB of Bcl2 and Bax. H. WB of EMT-related factors. I and J. Typical migration (I) and invasion (J) images of normoxia- and hypoxia-cultured cells. K. WB of NF $\kappa$ Bp65. \*\*p<0.01.

**Fig. 3** The regulatory relationship among NF $\kappa$ B, HIF1 $\alpha$  and HIF2 $\alpha$  were analysed in stably transfected GBM clones. A and B: NF $\kappa$ Bp65 expression (A) and  $\kappa$ B transcriptional activity (B) respectively in mock and NF $\kappa$ Bp65 transfected clones. C and D: HIF1 $\alpha$  expression (C) and HRE transcriptional activity (D) respectively in mock and HIF1 $\alpha$  transfected clones. E and F: HIF2 $\alpha$  expression (E) and HRE activity (F) respectively in

mock and HIF2 $\alpha$  transfected clones. G and H: HIF1 $\alpha$ , HIF2 $\alpha$  protein expression (G) and HRE activity (H) in mock and NF $\kappa$ Bp65 transfected clones. I and J: NF $\kappa$ Bp65 protein expression (I) and  $\kappa$ B activity (J) in mock and HIF1 $\alpha$  transfected clones. K and M: NF $\kappa$ Bp65 protein expression (K) and  $\kappa$ B activity (M) in mock and HIF2 $\alpha$  transfected clones. Clone C4 (red framed) was not used in this study. Reporter gene assay: mean  $\pm$  SD; n=3. \*\*p<0.01.

**Fig. 4** Analysis of EMT/stemness, cytotoxicity of TMZ and migration/invasion status in NF $\kappa$ Bp65, HIF1 $\alpha$  and HIF2 $\alpha$  transfected clones. A. Flow cytometric analysis of CD44, CD133 expression and ALDH activity (mean  $\pm$  SD; n=3). B and C. WB analysis of embryonic stem cell (B) and EMT-related (C) proteins. D. Real-time RT-PCR analysis of EMT and invasion-related genes. E. Cytotoxicity of TMZ (mean  $\pm$  SD; n=3). F, G, H. Representative migration/invasion images of HIF1 $\alpha$  (F), HIF2 $\alpha$  (G) and NF $\kappa$ Bp65 (H) transfected clones. \*p<0.05; \*\*p<0.01

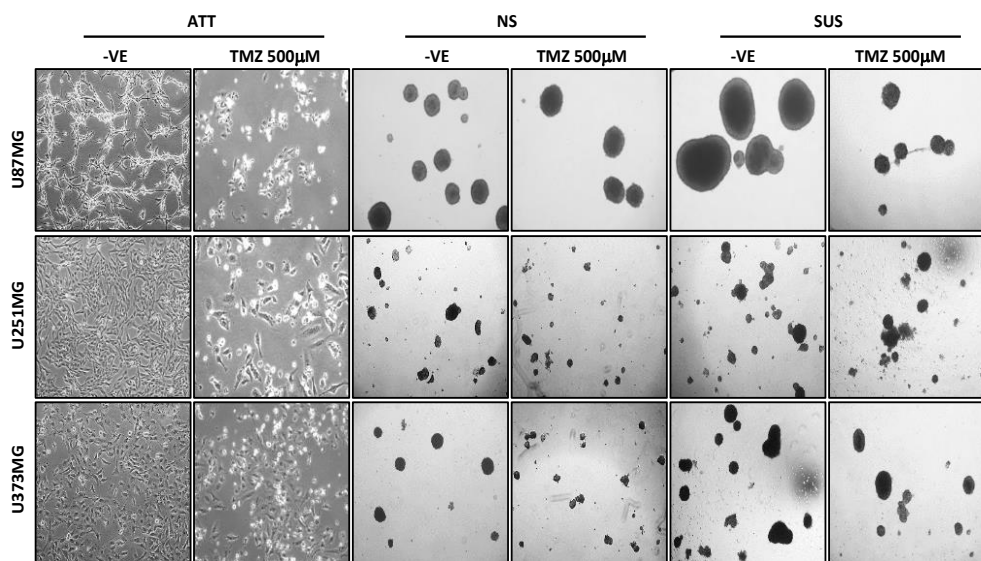
**Fig. 5** Analysis of the effect of DS/Cu on hypoxia-induced chemoresistance, EMT/stemness, invasiveness and NF $\kappa$ Bp65 expression. A. IC<sub>50s</sub> of DS/Cu in normoxia- and hypoxia-cultured cells (mean  $\pm$  SD; n=3). B and C: The effect of DS, Cu and DS/Cu on the sphere-reformation ability of NS (B) and SUS (C) cultured cells. D and E: Representative flow cytometric dot plots of the effect of DS/Cu on the ALDH activity (D) and CD133 expression (E). F and G: Effect of DS/Cu on the migration (F) and invasion (G) of the hypoxia-cultured GBM cell lines. H. WB analysis of the effect of DS/Cu on attached normoxia (ATT NOR), hypoxia (ATT HYP), NS and SUS culture induced NF $\kappa$ Bp65 protein expression.

**Fig. 6** Anti-GBM efficacy and selectivity of DS-PLGA/Cu in mouse GBM xenograft models. A. The fluorescent and pathological images of Anti-GBM efficacy of DS-PLGA/Cu on intracranial GBM model. B. The macrographic images of the effect of DS-PLGA/Cu on s.c xenografts. C. The s.c xenograft weight (mean  $\pm$  SD; n=7; \*\*p<0.01). D. TUNEL staining s.c xenograft. E. Immunohistochemistic analysis of NF $\kappa$ Bp65, Ki67 and ALDH

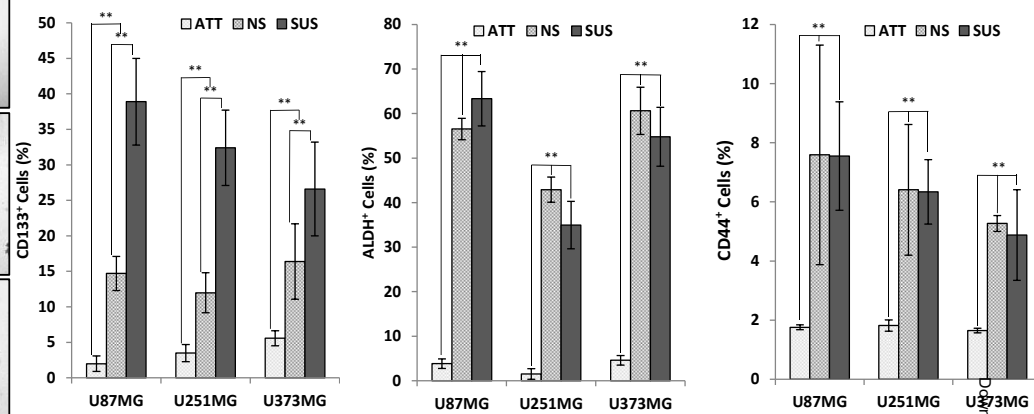
expression in s.c xenografts. F. The alteration of mouse body weight. G. The histological images of mouse organs.

Figure 1

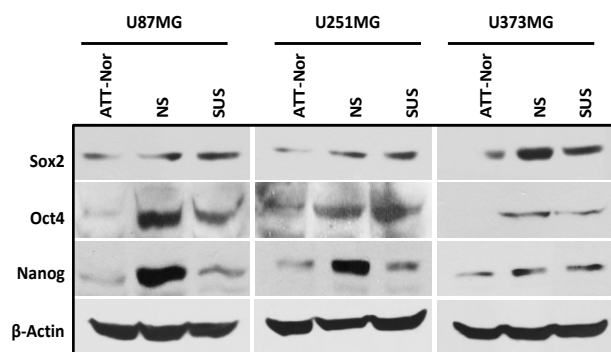
A



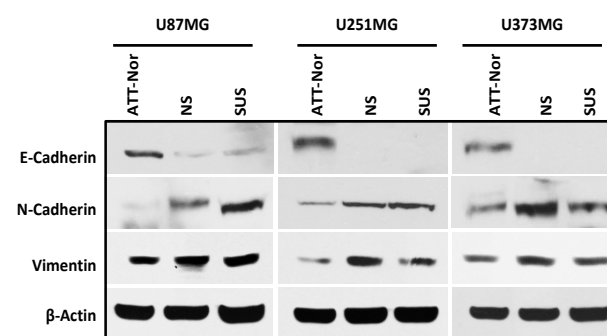
B



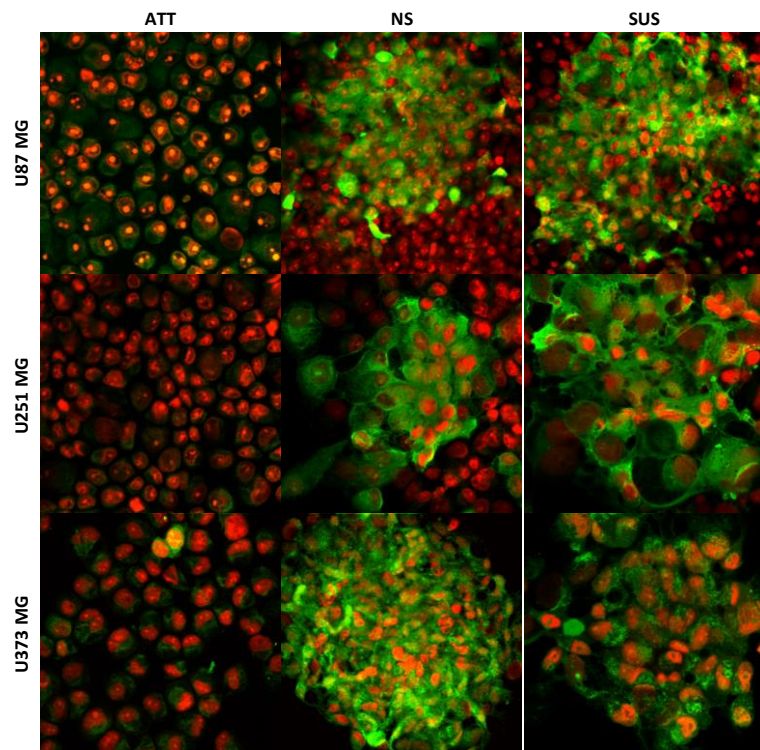
C



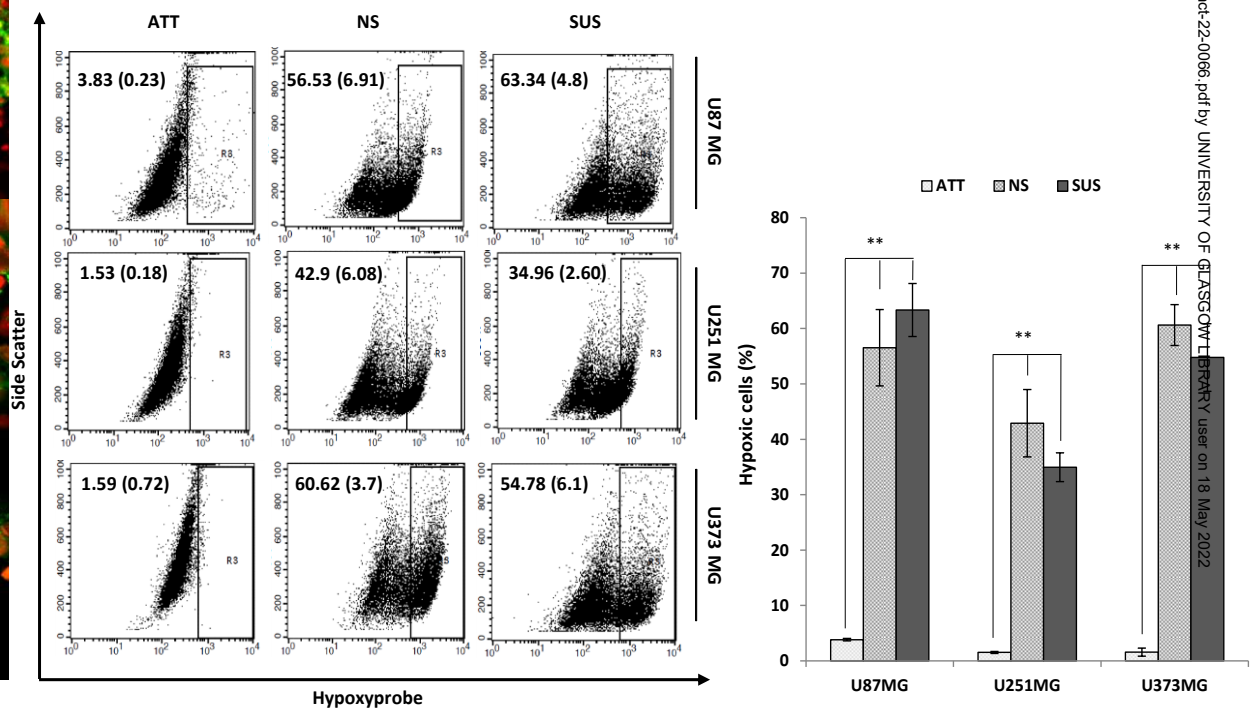
D



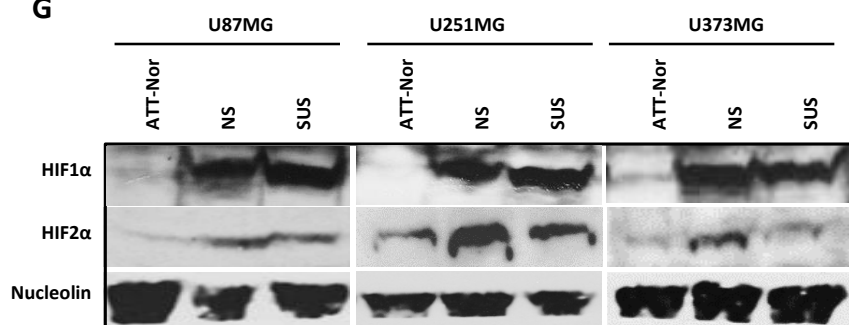
E



F



G



H

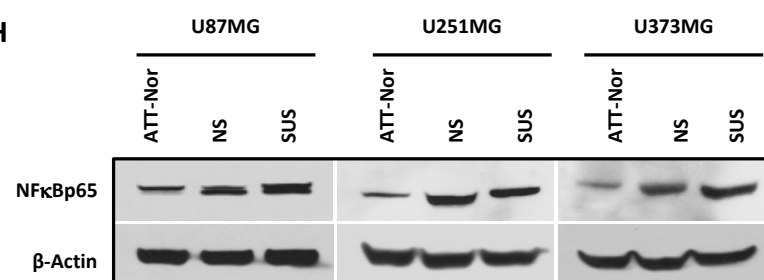
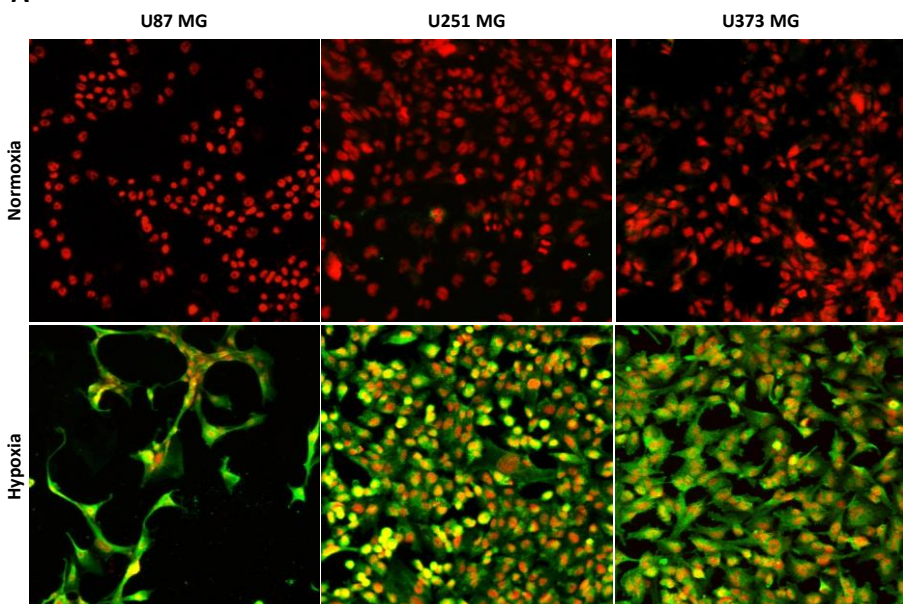
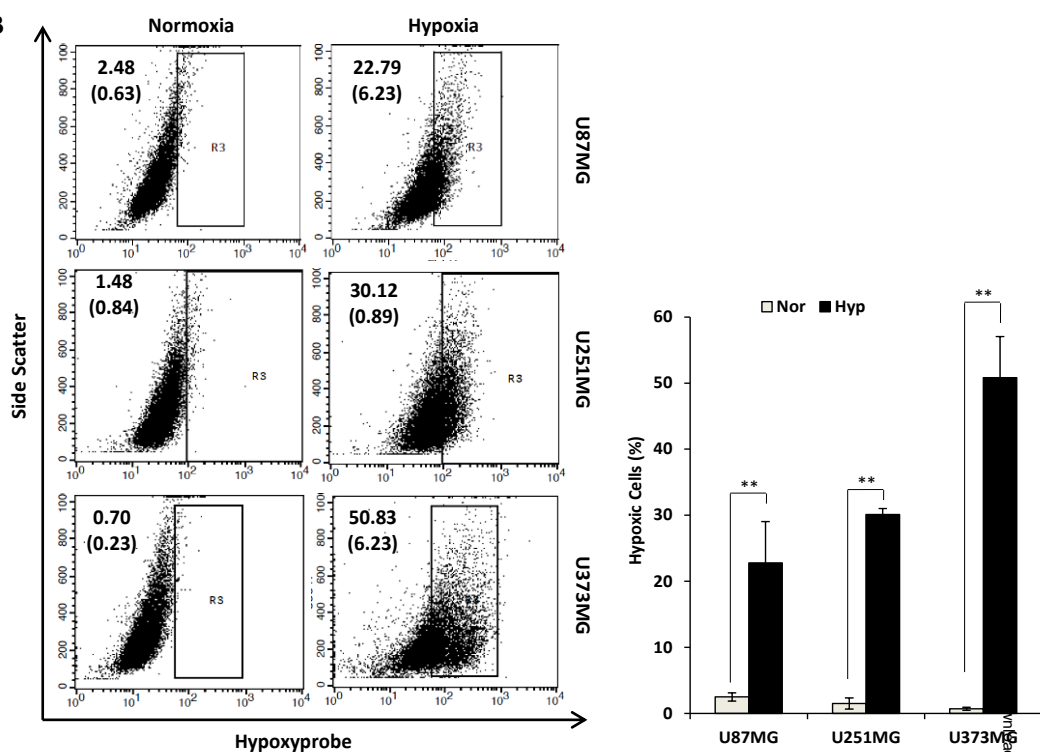


Figure 2

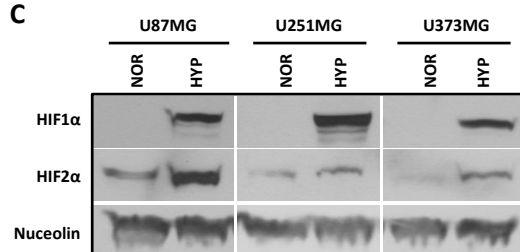
A



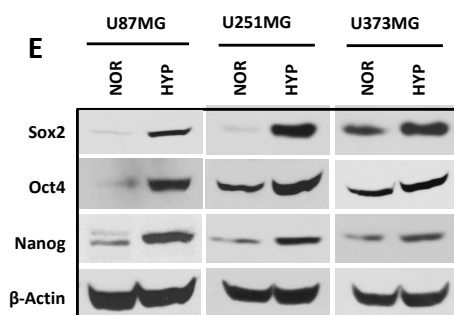
B



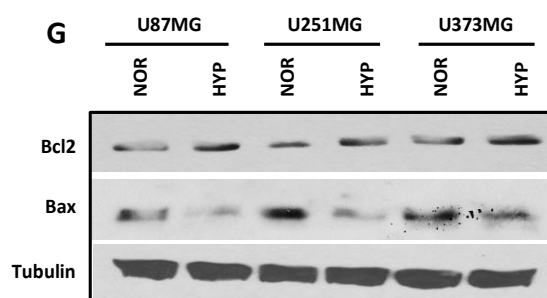
C



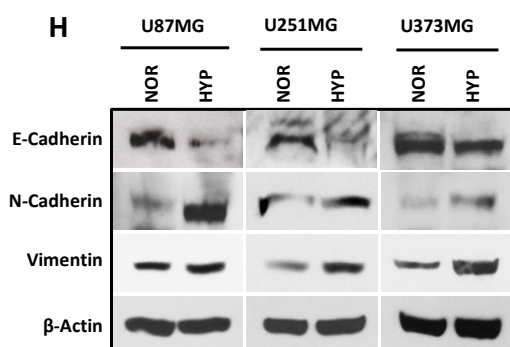
E



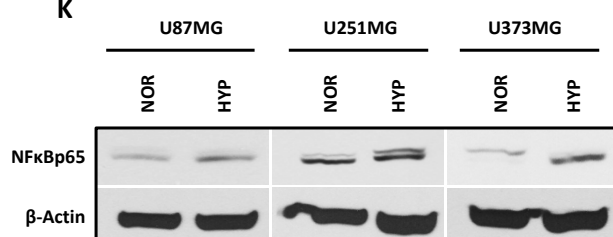
G



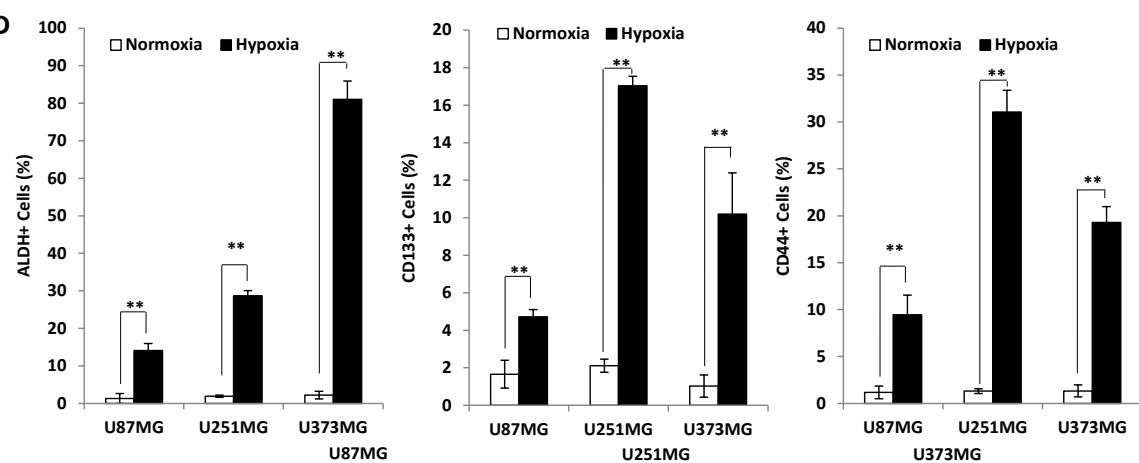
H



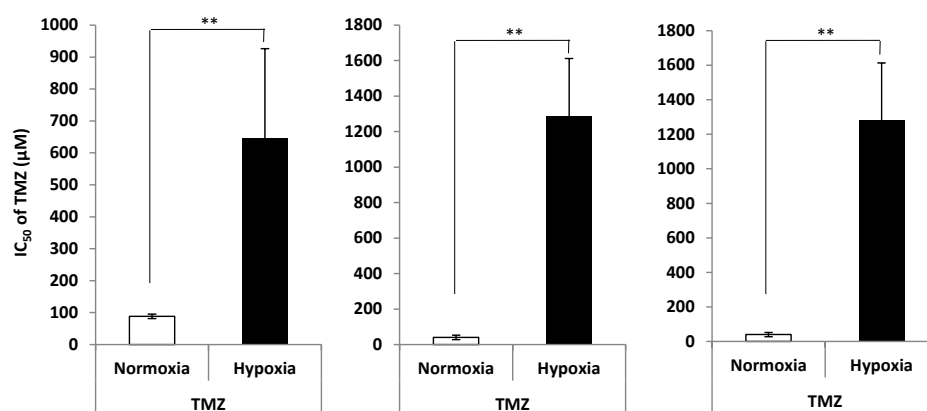
K



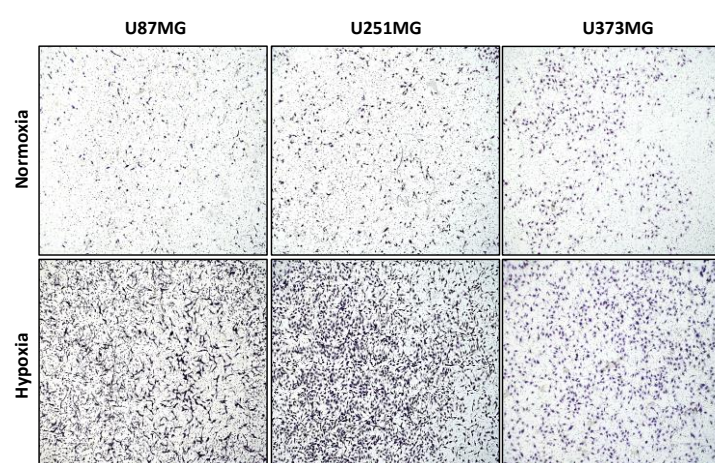
D



F



I



J

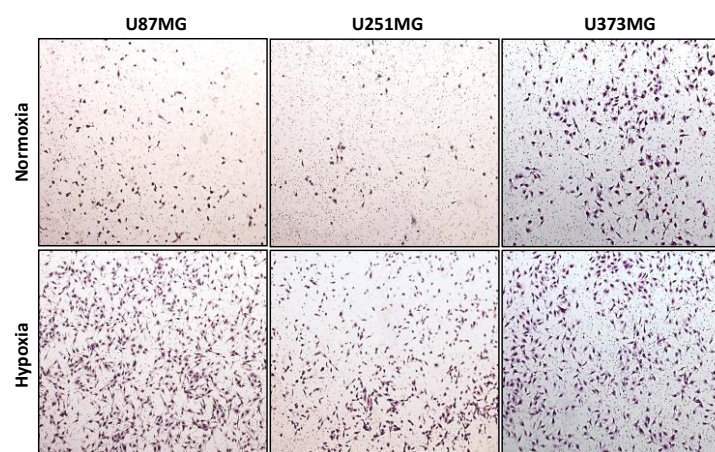


Figure 3

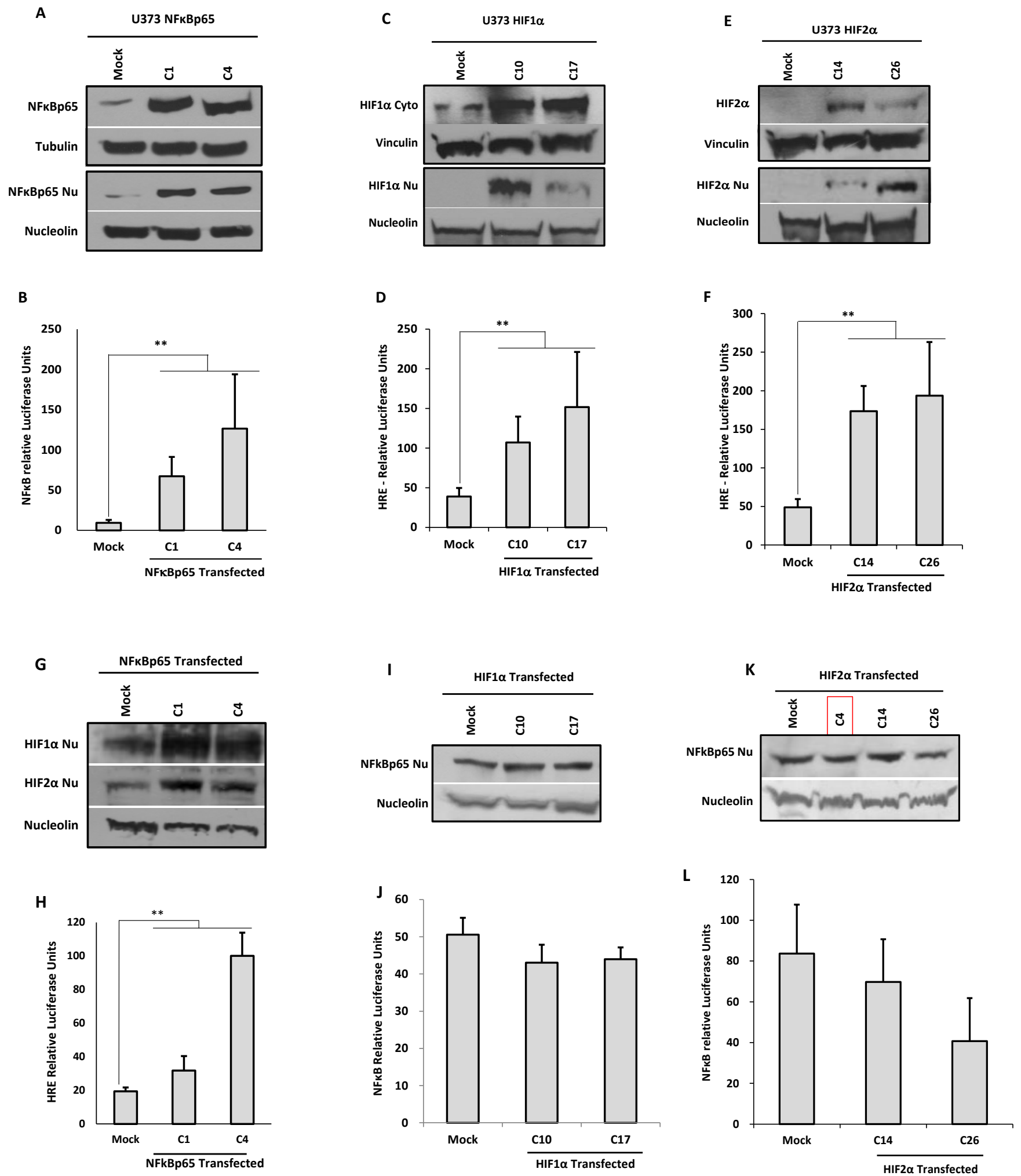
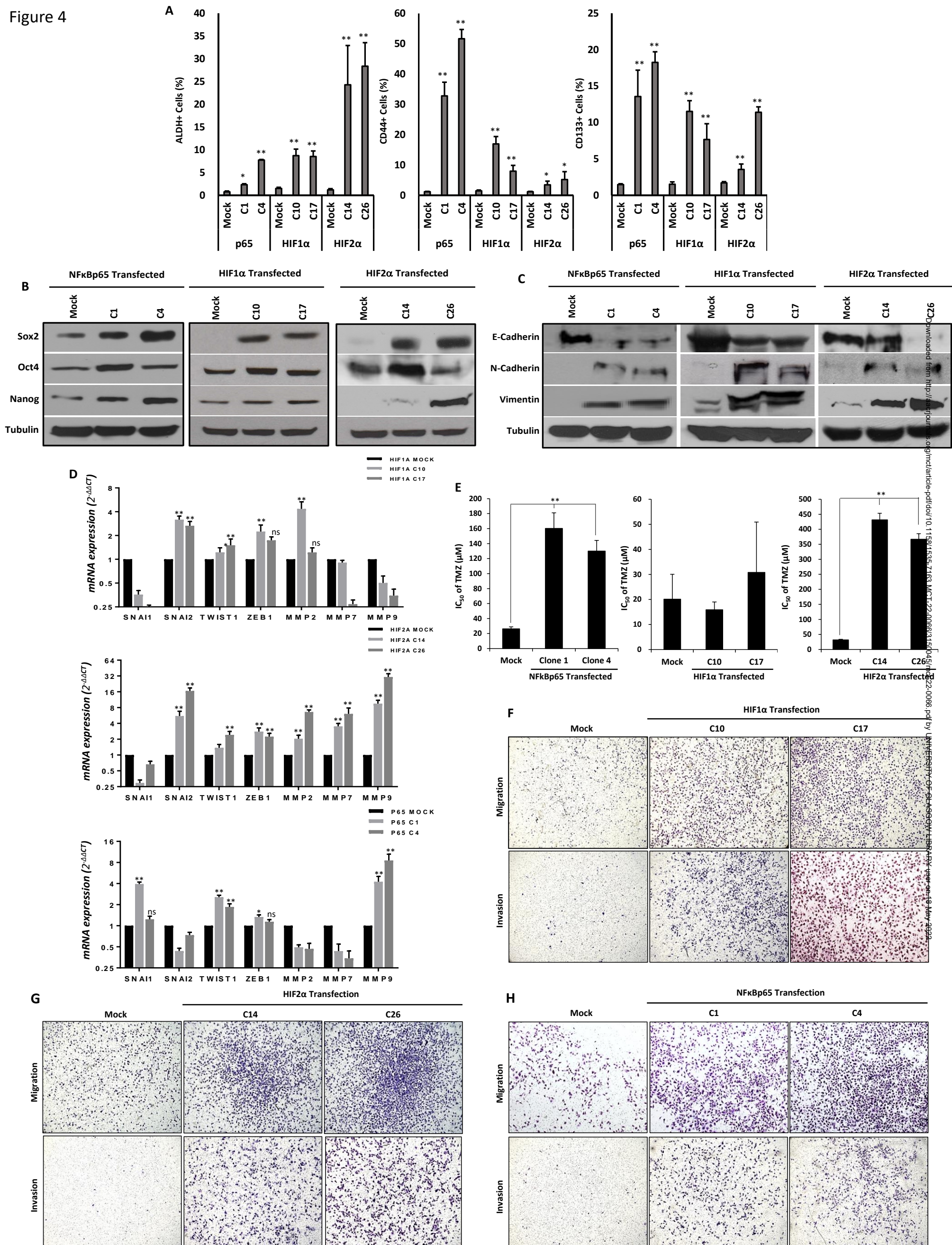


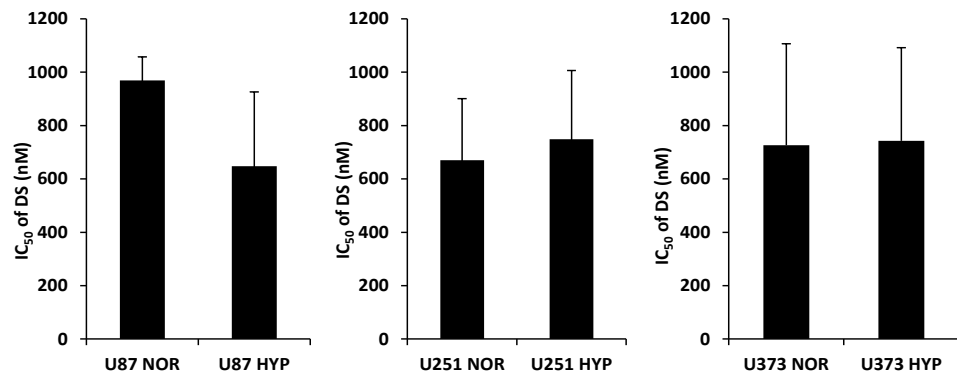
Figure 4



Downloaded from <http://ascipub.assp.org/> on May 10, 2015. For personal use only; all rights reserved.

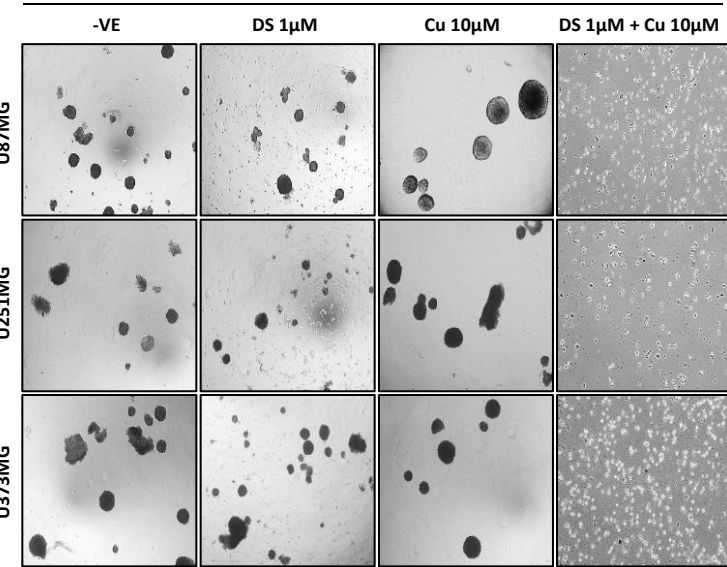
Figure 5

**A**

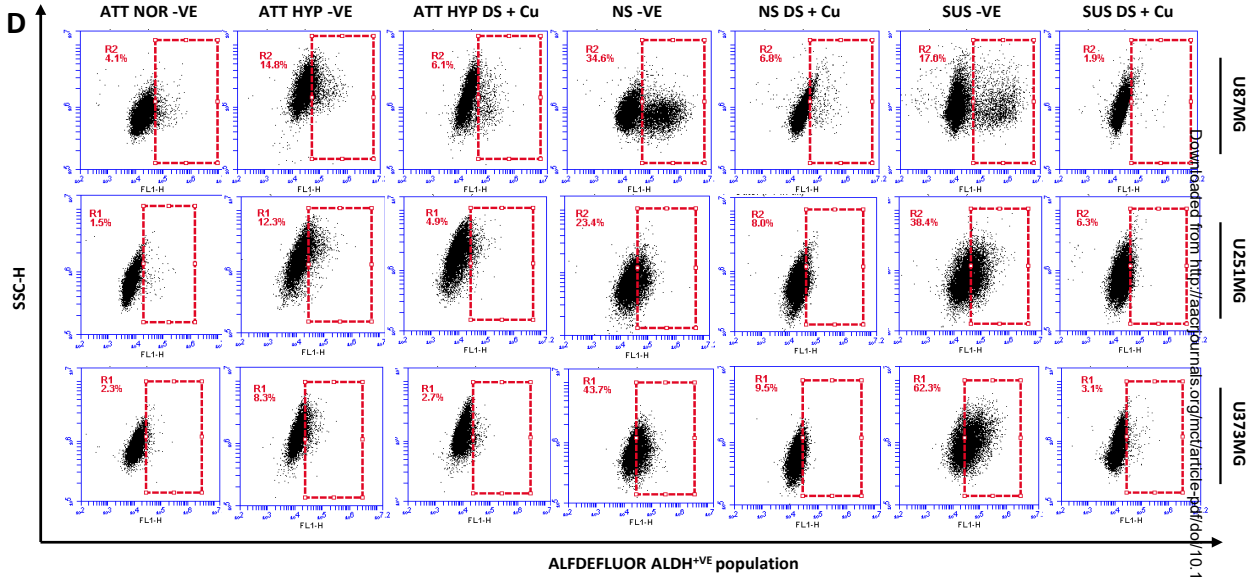


**B**

Neurosphere Cultured Cells

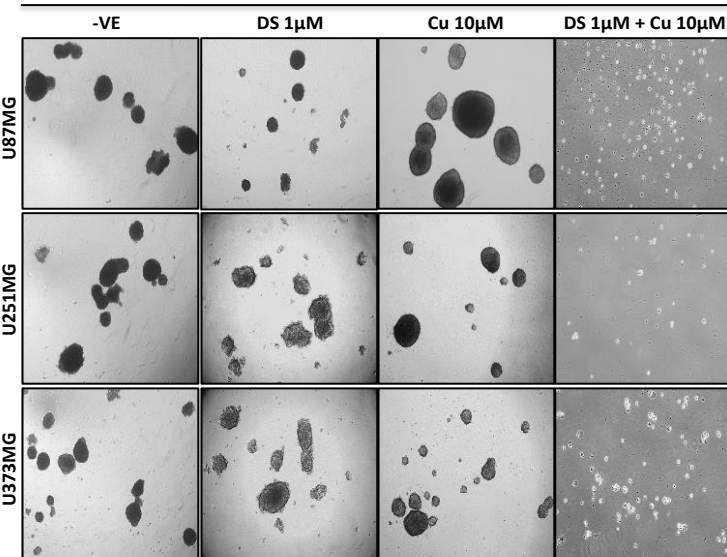


**D**

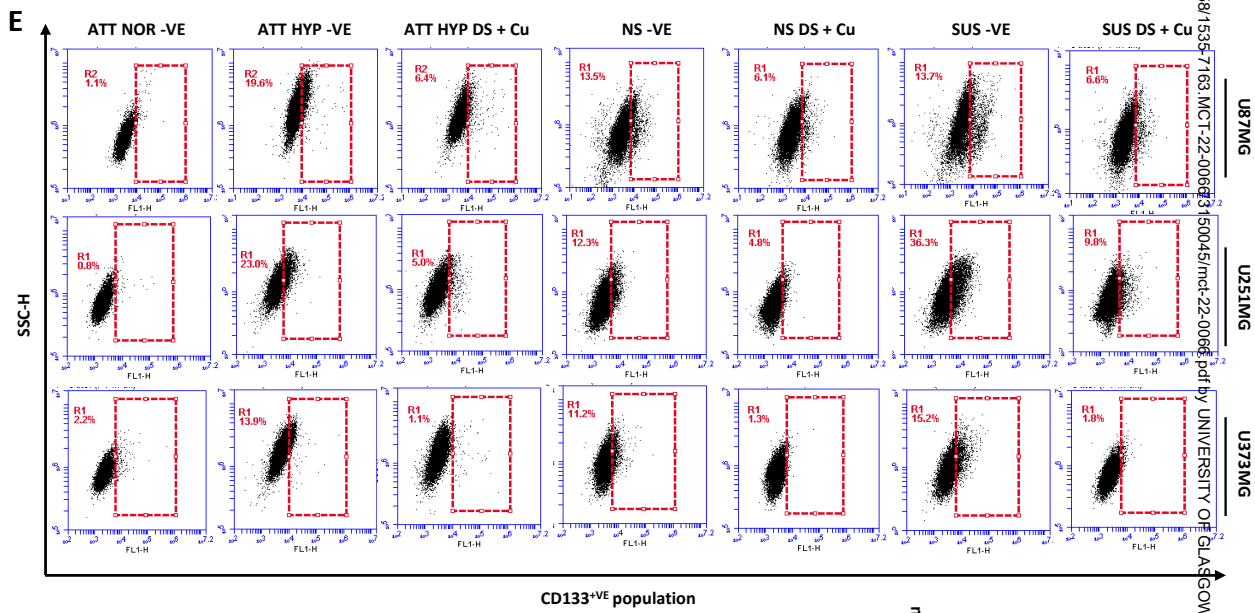


**C**

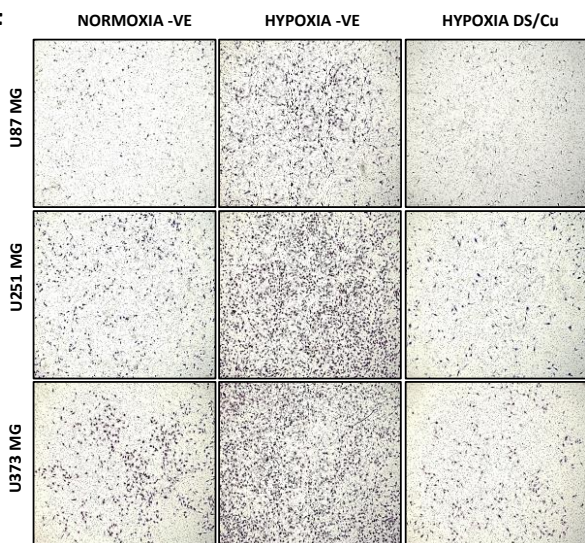
Suspension Cultured Cells



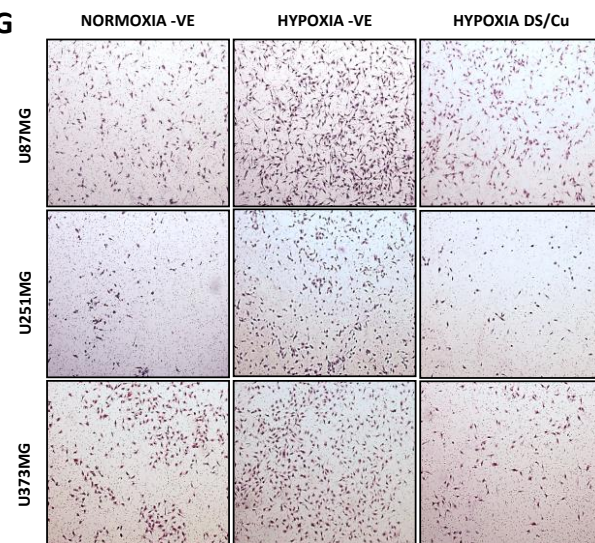
**E**



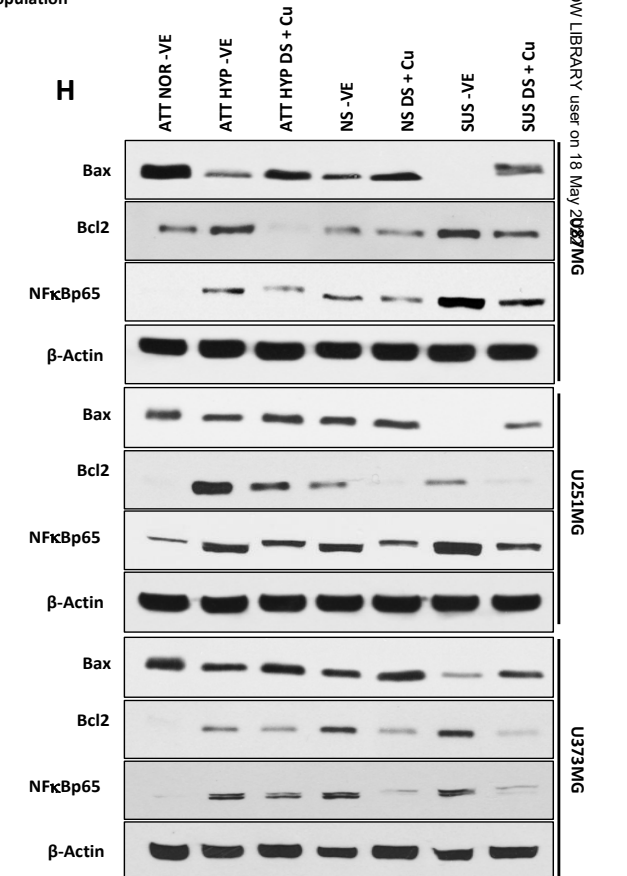
**F**



**G**



**H**



Downloaded from http://aacr.jco.org/ on May 18, 2015

Figure 6

